Eur. Phys. J. C (2025) 85:253
https://doi.org/10.1140/epjc/s10052-025-14000-8

THE EUROPEAN PHYSICAL JOURNAL C

Regular Article - Theoretical Physics

Dynamics of compact objects in higher-order curvature gravity using Finch–Skea spacetime

M. Ilyas[1,a], **Nehad Ali Shah**[2,b], **Fawad Khan**[1,c], **Rashid Habib**[1,d]

[1] Institute of Physics, Gomal University, Dera Ismail Khan 29220, KP, Pakistan
[2] Department of Mathematics and Statistics, College of Science, Imam Mohammad Ibn Saud Islamic University (IMSIU), 11623 Riyadh, Saudi Arabia

Received: 12 January 2025 / Accepted: 22 February 2025
© The Author(s) 2025

Abstract This paper explores anisotropic spherical structures within metric $f(R)$ gravity, where R is the Ricci scalar, extending general relativity to include functions of R modified gravitational effects. We analyze compact stars using Finch–Skea solutions under the models; $f(R) = R + \alpha R^2$, $f = R + \alpha R^2(1 + \gamma R)$, and $f = R + \alpha R\left(e^{-\frac{R}{\gamma}} - 1\right)$. These models help us examine how gravity modifications affect the internal structure and behavior of neutrons and strange stars. We investigate material variables such as density, pressures, anisotropy, and forces (gravitational, hydrostatic, anisotropic) through graphical analysis. The physical viability of the stellar models is assessed by evaluating energy conditions (NEC, WEC, SEC, and DEC) and the equation of state (EoS) parameter. We also examine the role of anisotropy in stability and structure, comparing the results with general relativity to highlight the implications of $f(R)$ gravity on compact stars. This study aims to enhance the understanding of how modified gravity theories could impact the properties of compact astrophysical objects.

1 Introduction

The basis of modern cosmology was established by general relativity (GR). The physical aspects of the Λ-cold dark matter model exhibit different characteristics, such as fine-tuning and cosmic coincidence. Still, overall they are consistent with all cosmological scenarios [1–3]. Microwave radiations, large-scale structures, supernovae Type Ia surveys, and the decreased energy flux through cosmic backgrounds in Redshift all show that the universe is expanding more quickly than expected [4–6]. These results have indicated that this intriguing and puzzling phenomenon is caused by the enigmatic element known as dark energy (DE). These changes to Einstein's gravity have been proposed in a number of ways. The work [7] suggested altering relativistic dynamics to solve cosmic issues such as dark matter and quantum gravity.

The gravitational component of the GR action is the only part of the generalized models that underwent modification to construct the modified theories of gravity. The first observationally and theoretically possible scenario of our accelerated universe was proposed by Nojiri and Odintsov using $f(R)$ gravity [8]. Recent research by [9] has examined a variety of cosmic issues, such as cosmic acceleration and bouncing cosmology in the early and late times. According to them, a number of intriguing cosmic scenarios might be demonstrated by simulating extended gravity theories such as $f(R)$, $f(T)$ (Torsion Scalar), and $f(G)$ (Gauss-Bonnet term).

The fundamental mechanism underlying many fascinating phenomena, such as phase transitions of distinct kinds [10], pion condensation [11], the presence of both a solid and a Minkowskian core [12–16], etc., is the investigation of anisotropic effects on compact object matter structures. For a static isotropic relativistic collapsing cylinder, all feasible precise solutions may be expressed in terms of scalar expressions, both in general relativity [17] and $f(R)$ gravity [18,19]. Sussman and Jaime [20] examined a group of atypical spherical solutions where a traceless anisotropic pressure tensor was present to select a model where $f(R) \propto \sqrt{R}$. A recent extension of $f(R, T)$ gravity incorporating unimodular constraints has been proposed by Rajabi and Nozari, which may offer new insights into the field equations and cosmological implications [21]. The stability of a growing

[a] e-mail: ilyas_mia@yahoo.com (corresponding author)
[b] e-mail: nashah@imamu.edu.sa (corresponding author)
[c] e-mail: fawad.ccms@gmail.com
[d] e-mail: habib786070@yahoo.com

Published online: 10 March 2025

Einstein universe was examined by Shabani and Ziaie in relation to the dynamical and computational consequences of a particular $f(R, T)$ gravity model. According to the work of [22], which looked at a number of stable configurations of different anisotropic relativistic compact objects, different compact star forms are likely maintained by extra curvature gravitational forces that come from gravity's rainbow. Numerous cosmological features were investigated in a framework of anisotropic relativistic backgrounds by Sahoo et al. [23,24].

An intriguing mechanism known as gravitational collapse (GC) allows star bodies to constantly drift nearer their centers of mass. According to the singularity theorem [25], spacetime singularities might occur in the domain of Einstein's gravity in the act of enormous relativistic structures collapsing. Several relativistic astrophysicists and gravitational theorists have expressed an avid curiosity about studying the final stellar phase. In this regard, many publications [26–29] investigated the GC issue using a few possible matter and geometry configurations. Regarding collapsing star interiors and black holes, various outcomes have been obtained in the scientific literature under the f (R) gravity framework [30–33].

By applying a perturbation technique to evaluate dispersion expressions, Capozziello et al. [34,35] examined the gravitational collapse of non-interacting particles and discovered an unstable zone within the collapsing object at specific boundaries. Cembranos et al. [36] examined the large-scale evolution of nonstatic inhomogeneous gravitational resources in various $f(R)$ gravity models. Huge stellar objects with lower radii than GR will probably be found under modified gravity theories [37–39]. Considering a spherically symmetric spacetime with a scalar GC, Guo, and Joshi [40] deduced that black hole structures might arise from a relativistic sphere under intense source field conditions.

It is possible to think of the idea of energy conditions (ECs) as a workable strategy for comprehending the well-known singularity theorem. Viability constraints derived from ECs were obtained by Santos et al. [41] using a general $f(R)$ formalism. Several potential $f(R)$ gravity models may be restricted by the way they work. After evaluating ECs for $f(R)$ gravity, Shiravand et al. [41] were able to extract certain stability limits regarding Dolgov–Kawasaki instability. They discovered unique phases for a few $f(R)$ parameter values, within which the theory would meet WECs. This work's primary objective is to examine the role that anisotropic pressure and $f(R)$ models play in simulating actual compact star formations. We examine a wide range of structural aspects for three distinct stellar structure observational data sets, including energy conditions, stability, pressure distributions, anisotropic density, the Tolman–Oppenheimer–Volkoff (TOV) equation, and the EOS parameters.

The structure of the paper is outlined as follows: in the next section, we provide a concise review of $f(R)$ gravity for anisotropic matter distributions in static spherical geometry. Section 3 discusses the anisotropic distribution of matter in $f(R)$ gravity, while Sect. 4 focuses on complementing Schwarzschild s external metric. Various $f(R)$ gravity models are explored in Sect. 5. In Sect. 6, we analyze the physical features of these models, including the viability of three key star formation scenarios. The paper concludes with a summary of our main findings.

2 $f(R)$ gravity

An extension of the conventional Einstein–Hilbert action employed in general relativity is utilized to formulate the action in modified $f(R)$ gravity theories. These theories use a function that is a Ricci scalar, represented as $f(R)$, rather than the Ricci scalar R alone. The action can be expressed as follows:

$$I = \int d^4x\sqrt{-g}\,[f(R) + \mathcal{L}_m] \tag{1}$$

The expression is the mathematical framework of modified gravity theories of how several key components that work together to describe the basic quantitative relations between spacetime and matter behave. Here $\sqrt{-g}$ is the negative square-root of determinant of metric tensor $g_{\mu\nu}$. A generalized gravity function, $f(R)$, is used, which describes generic gravitational dynamics beyond the familiar range of general relativity, giving it the freedom to exhibit more and more complicated behaviors. $\mathcal{L}_m$ contains all the matter and energy included in the universe, the interactions among them, and the contribution of all these to the understanding of full gravitational dynamics.

This action encapsulates the essence of modified gravity theories by providing a mechanism to alter the fundamental interactions of gravity without strictly adhering to the linear dependence on R as in general relativity.

Modified $f(R)$ gravity field equations

Variation of the action according to the metric tensor $g_{\mu\nu}$ allows one to obtain the field equations governing spacetime dynamics in modified $f(R)$ gravity. This change results in the following modified Einstein equations:

$$f_R R_{\mu\nu} - \frac{1}{2}g_{\mu\nu}f(R) + \left(g_{\mu\nu}\Box - \nabla_\mu\nabla_\nu\right)f_R = T_{\mu\nu} \tag{2}$$

where $f_R(R)$ is the derivative w.r.t. Ricci scalar, R, as $f_R = \frac{df(R)}{dR}$, which further adds scalar degrees of freedom. The Ricci curvature tensor $R_{\mu\nu}$ measures spacetime

curvature caused by matter and energy. The d'Alembertian $\Box = \nabla^\alpha \nabla_\alpha$ a covariant derivative to make curvature good depends on spacetime. The energy momentum tensor, or $T_{\mu\nu}$, characterizes the matter and energy distribution in spacetime.

The terms involving f_R and its derivatives introduce corrections to the usual Einstein field equations, resulting in modified dynamics. Without the necessity for a cosmological constant, these changes may result in phenomena like the cosmos expanding more quickly.

Tensor of energy–momentum for a fluid

The tensor of energy–momentum $T_{\mu\nu}$, which shows how matter and energy affect spacetime's curvature, is a crucial part of the field equations. The general expression for the fluid's energy–momentum tensor is as follows:

$$T_{\mu\nu} = (\rho + P_r)U_\mu U_\nu - P_t g_{\mu\nu} + (P_r - P_t)V_\mu V_\nu \tag{3}$$

where each term plays a distinct role in describing the system. The energy density ρ represents the amount of energy per unit volume as measured in the fluid's rest frame. The radial pressure P_r acts along the radial direction, while the tangential pressure P_t acts perpendicular to it. The four-velocity U_μ describes the motion of the fluid and satisfies the normalization condition $U_\mu U^\mu = 1$, ensuring proper relativistic behavior. The metric tensor $g_{\mu\nu}$ encodes the geometry of spacetime, while the radial unit vector V_μ, with $V_\mu V^\mu = -1$, is used to describe anisotropic contributions in the radial direction.

This formulation of the tensor of energy–momentum matter distribution allows for a more general description of fluids, including cases where pressures differ in different spatial directions. This is particularly useful in modeling astrophysical objects like anisotropic stars or considering cosmological models where anisotropic stress may play a role.

Section 3 builds upon the formalism established in Sect. 2 by applying the modified field equations to a spherically symmetric anisotropic matter configuration. The analysis focuses on how these equations affect the internal structure of compact stars, where the presence of anisotropy characterized by differences in radial and tangential pressures plays a critical role. Solving the equations in this context yields explicit expressions for the energy density, radial pressure, and tangential pressure. These quantities, determined by the specific form of $f(R)$ and its derivatives, provide insight into how the behavior of matter within dense astrophysical objects is influenced by the modified gravity framework. Subsequent sections further extend this analysis by exploring additional physical scenarios and implications of $f(R)$ gravity.

3 Anisotropic distribution of matter in $f(R)$ gravity

Understanding how gravity variations can impact the stability and internal structure of compact stars is possible through the examination of anisotropic matter distributions in these objects under $f(R)$ gravity. For spherically symmetric geometry, the line element is provided by:

$$ds^2 = e^{a(r)}dt^2 - e^{b(r)}dr^2 - r^2(d\theta^2 + r^2\sin^2\theta\, d\phi^2), \tag{4}$$

where the gravitational potential is described in the radial and time frame directions by the metric functions $e^{b(r)}$ and $e^{a(r)}$ correspondingly. The modeling of stellar compact objects using Finch–Skea solutions has gained a lot of interest in recent years due to their non-singular behavior. The Finch–Skea metric functions are defined in [42] as:

$$e^{a(r)} = \left(A + \frac{1}{2}B\sqrt{Cr^2}\right)^2, \tag{5}$$

which represents the gravitational potential in the temporal component, and

$$e^{b(r)} = 1 + Cr^2, \tag{6}$$

corresponding to the spatial curvature influenced by the matter distribution. The Finch–Skea spacetime is a well-regarded interior solution of Einstein s field equations, originally developed to model static, spherically symmetric stellar configurations with anisotropic matter distributions. It has found extensive applications in modeling compact stars, including neutron stars, due to its physically realistic properties such as regularity at the center, positive-definite pressure, and density profiles that decrease monotonically towards the boundary. One of the key reasons for employing the Finch–Skea metric in the context of compact stars is its adaptability to both relativistic and modified gravity theories, including $f(R)$ gravity. The metric exhibits properties that align well with the requirements of modified theories, allowing for the exploration of deviations from standard general relativity while maintaining physically acceptable stellar models. Specifically, the Finch–Skea spacetime enables the analytical treatment of the modified field equations, providing insights into the effects of curvature corrections and higher-order terms inherent in $f(R)$ gravity. Moreover, the use of Finch–Skea geometry allows for the imposition of realistic boundary conditions at the stellar surface, which is crucial in determining the stability and equilibrium of the stellar configuration. Its simplicity, combined with its physical relevance, makes it an ideal candidate for investigating the anisotropic nature of compact stars and their behavior under gravitational modifications.

In the present study, the Finch–Skea spacetime has been chosen to explore the effects of $f(R)$ gravity corrections on the internal structure and stability of compact stellar objects. By employing this metric, we aim to provide a comprehensive analysis of the equilibrium configurations and energy conditions that govern such systems, offering new insights into the behavior of self-gravitating objects within the framework of modified gravity theories.

The constants A, B, and C are found by applying boundary constraints, like comparing the interior solutions to an external vacuum solution, like the Schwarzschild metric at the star's surface.

These metric functions are combined with the modified field equations from Sect. 2 to produce formulae for the tangential pressure (P_t), radial pressure (P_r), and energy density (ρ):

$$\begin{aligned}\rho =& \frac{e^{-a}}{2r^2}\\ &\times\left(r^2a'f_R'+2f_Rra'+f(-r^2e^a)+f_Rr^2e^aR\right.\\ &\left.+2f_Re^a-2r^2f_R''-4rf_R'-2f_R\right),\end{aligned} \tag{7}$$

$$\begin{aligned}P_r =& -\frac{e^{-a}}{2r^2}\\ &\times\left(-2f_R+2e^af_R-e^af_Rr^2+e^af_Rr^2R\right.\\ &\left.-2f_Rrb'-4rf_R'-r^2b'f_R'\right),\end{aligned} \tag{8}$$

$$\begin{aligned}P_t =& \frac{e^{-a}}{4r}\\ &\times\left(2f_Rrb''-f_Rrb'a'+2rb'f_R'+f_Rrb'^2\right.\\ &+2f_Rb'-2ra'f_R'-2f_Ra'\\ &\left.+2rfe^a-2rf_Re^aR+4rf_R''+4f_R'\right).\end{aligned} \tag{9}$$

The Ricci scalar, R, for this metric is given by:

$$R=\frac{e^{-b}}{2r^2}\left(4-4e^b+r^2a'^2-4rb'+ra'(4-rb')+2r^2a''\right).$$

Here, the prime symbol ($'$) denotes differentiation with respect to the radial coordinate r. The curvature terms and their changes from $f(R)$ gravity affect the distribution of energy and pressure within the star, as shown by these expressions for ρ, P_r, and P_t. The radial and tangential pressures in anisotropic models are not equal ($P_r \neq P_t$), which results in a pressure anisotropy that is defined by the difference $P_t - P_r$. In contrast to general relativity's isotropic models, this anisotropy may have a substantial impact on the star's stability and structure, altering its equilibrium and possibly producing distinct physical results.

The dependence of these quantities on f_R and its derivatives reflects the broader dynamics introduced by $f(R)$ gravity, including possible deviations from the predictions of general relativity. These deviations can manifest in various astrophysical phenomena, such as the potential for greater compactness, altered mass-radius relations, and different stability criteria for the star. Investigating these effects is essential to comprehending the entire spectrum of potential compact object behaviors under altered hypotheses of gravity.

Overall, the modified field equations derived earlier are thoroughly applied to a physically relevant astrophysical scenario, highlighting how changes in gravity affect the interior structure of anisotropic compact stars. This analysis plays a crucial role in understanding the theoretical consequences and potential observational signatures of $f(R)$ gravity, particularly concerning star evolution and internal dynamics.

4 Complementing Schwarzschild's external metric

To understand the transition from the interior metric of a spherically symmetric body to the exterior region, we need to match it to the Schwarzschild exterior metric. This matching process ensures that the metric is continuous across the boundary of the object, typically a star or planet, and that the spacetime is smooth and well-behaved.

According to the Schwarzschild metric, the exterior solution is the spacetime outside of a spherically symmetric, non-rotating, uncharged mass:

$$\begin{aligned}ds^2 =& \left(1-\frac{2M}{r}\right)dt^2-\left(1-\frac{2M}{r}\right)^{-1}\\ &\times dr^2-r^2\left(d\theta^2+\sin^2\theta\,d\varphi^2\right)\end{aligned} \tag{10}$$

M is the total mass of the object in the gravitational fields, and in celestial objects just is $G = c = 1$. r stands for the radial distance from the object's center point. The rest coordinates of T for time measurement and then θ and φ for angular coordinates to specify positions on three-dimensional space.

To ensure a consistent stellar model, we consider a three-dimensional hypersurface Σ that separates the system into interior and exterior regions. The interior is described by the Finch–Skea spacetime, and the continuity of the structural variables, i.e., g_{ii} (for $i = 1, 2$), and the derivative $\partial g_{tt}/\partial r$ across the hypersurface $r = R$, provides essential junction conditions. These junction conditions provide a system of equations that, when solved simultaneously, determine the constants A, B, and C. This smooth transition ensures the physical validity of the stellar model under $f(R)$ gravity.

1. The parameter A is established as follows:

$$A=\frac{2R-5M}{2\sqrt{R}\sqrt{R-2M}} \tag{11}$$

This parameter involves both the radius R and the mass M and is related to the gravitational potential near the surface of the object.

2. The parameter B is established as follows:

$$B = \frac{\sqrt{\frac{M}{R-2M}}\sqrt{R-2M}}{\sqrt{2}\,R^{\frac{3}{2}}} \tag{12}$$

This expression combines terms involving the radius R, mass M, and a term m, which may represent an interior mass distribution parameter. This term ensures the proper scaling of the metric components inside and at the boundary.

3. The parameter C is established as follows:

$$C = \frac{2M}{R^2(R-2M)} \tag{13}$$

This parameter represents the effect of the mass M on the curvature of space at the surface radius R. It plays a crucial role in ensuring the continuity of the radial component of the metric across the boundary.

The correct matching of these parameters guarantees that both the interior and exterior solutions describe a single, coherent spacetime geometry. This is important in general relativity, as it allows for a realistic description of the gravitational field around astrophysical objects. The Schwarzschild solution thus serves as the canonical exterior solution for such spherically symmetric mass distributions.

5 Different models

This section will review some of the viable models for studying several properties of compact stars, including mass and energy conditions.

5.1 Model 1

Let's consider a model defined by a power-law dependence of the Ricci scalar, as discussed in [45], with α being a constant. Starobinsky originally proposed this model to illustrate the exponential growth of the universe's expansion during its early stages. In numerous studies, this specific formulation of the Ricci scalar is considered a plausible candidate for dark energy. Einstein's general theory of relativity is reached by the model at the limit when $f(R) \to R$.

$$f = R + \alpha R^2 \tag{14}$$

in which α is an arbitrary constant and R is the Ricci scalar. We can recover G.R for setting α equal to zero.

5.2 Model 2

We then consider the exponential gravity model based on the Ricci scalar, as outlined in [46], where the constants α and γ (model parameters) are introduced. These types of models have been thoroughly examined in cosmological contexts, as mentioned in [47]. Investigating this model provides a valuable framework for exploring the late-time acceleration of the universe while also being consistent with eras dominated bmatter,

$$f = R + \alpha R\left(e^{(-R/\gamma)} - 1\right) \tag{15}$$

in which α and γ are the two arbitrary constants.

5.3 Model 3

One might find it interesting to examine $f(R)$ adjustments of the type in which α and γ are independent constants. This model is particularly interesting because of the constraint $\gamma R \sim O(1)$, which enables a comparison between the analysis of a quadratic Ricci term and that of cubic Ricci scalar corrections,

$$f = R + \alpha R^2\,(1 + \gamma R) \tag{16}$$

in which the arbitrary constants are α and γ.

In our study, we adopted parameter values $\alpha = 0.03$, $\beta = 0.3$, and $\gamma = 0.5$ for the $f(R)$ gravity models. These values were selected to ensure the physical consistency of our compact star models while adhering to observational and experimental constraints. Small values of α, such as $\alpha = 0.03$, are consistent with solar system experiments, including perihelion precession, light deflection, and radar echo delays, which place stringent bounds on deviations from general relativity in weak-field regimes. The parameter $\gamma = 0.5$, governing the exponential correction in Model 2, ensures smooth suppression of high curvature effects without violating energy conditions or causing instabilities. In Model 3, the term $(1 + \gamma R)$ introduces higher-order curvature corrections, with $\beta = 0.3$ chosen to limit the correction strength and maintain consistency with known physical behaviors. These parameter values are also tuned to ensure stability, avoid ghost instabilities, and satisfy energy conditions across all models. By keeping the parameters within ranges supported by solar system and cosmological observations, our models maintain compatibility with well-tested regimes of general relativity while effectively capturing the behavior of compact stars under modified $f(R)$ gravity.

From this model, we derive ρ, P_r, and P_t using Eqs. (7–9), we verify the different features of compact stars as shown in Table 1. Each of these elements will be discussed separately in the next section.

6 Physical features of models of $f(R)$ gravity

Several established and feasible $f(R)$ gravity models are examined in this section to characterize the physical environments present in compact stellar interiors. Three distinct

Table 1 Approximate values for the mass M, radius R, and constants A, B, and C of the compact stars Her X-1, SAX J1808.4-3658, and 4U 1820-30

Star type	Mass (M)	Radius (km)	A	B	C
Her X-1	$0.88M_{\odot}$ [43]	7.7 [43]	0.711777	0.0376399	0.00853473
SAX J1808.4-3658	$1.44M_{\odot}$ [43]	7.07 [43]	0.398243	0.0546892	0.0297602
4U 1820-30	$2.25M_{\odot}$ [44]	10.0 [44]	0.293278	0.0407431	0.0197619

$f(R)$ models are used to investigate the evolution of pressure, energy density, the Tolman–Oppenheimer–Volkoff (TOV) equation, the equation of state parameter, and the energy conditions for three particular stars. With masses of $0.88M_{\odot}$, $1.435M_{\odot}$, and $2.25M_{\odot}$, respectively, the studied stellar configurations are Her X-1, SAX J1808.4-3658, and 4U 1820-30. Using the $f(R)$ models given in Eqs. (7–9), we investigate the stability features of compact stellar structures and determine ρ, p_r, and p_t, from which these values can be derived. After that, we will create various plots to examine how these stellar interiors behave. The designations CS1, CS2, and CS3 are assigned to Her X-1, SAX J1808.4-3658, and 4U 1820-30, respectively, as shown in these diagrams.

It is commonly accepted for defining quark structures composed of strange quark matter, known as strange compact stars. Theoretical evidence is large that quark stars might be forms of the neutron star remnants [48] or as a result of intense supernova explosions. Additionally, such structures may have actually come about in the beginning epochs of the universe, soon after the Big Bang [49]. However, the final act of stellar evolution, whether they are blackholes, neutron stars, or white dwarfs, is determined by their initial mass. Compact stars, which consist of these objects combined, are collectively known as compact stars. In the framework of a static, spherically symmetric relativistic structure that interacts with an ideal matter distribution, we formulate the upper bound on the mass to radius ratio in terms of $\frac{2M}{R} < \frac{8}{9}$. Such a relationship, called the Buchdahl–Bondi bound [26,50,51], has engendered much interest in relativistic astrophysicists studying compact objects. We perform an analysis of radial and transverse sound speeds in this paper. In addition, we will take into account the impacts of gravitational, hydrostatic, and anisotropic forces in potential modeling of compact stars in order to examine equilibrium circumstances. Furthermore, in order to investigate equilibrium conditions, we will consider the effects of gravitational, hydrostatic, and anisotropic forces in the potential modeling of compact stars.

6.1 Evolutions of pressure and energy density

The strange star candidates Her X-1, SAX J 1808.43658 (SS1), and 4U 1820-30 have density plots of ρ increasing as $R \to 0$, as seen in Fig. 1. Essentially, the ρ is comparable to the reducing function of r; that is, as r rises, ρ falls. This implies a very compact core of the star, validating the viability of our theories in $f(R)$ under study for the outer region of the core.

Likewise, the two other panels in Figs. 2 and 3 illustrate the fluctuation of the anisotropic traverser and radial pressures, p_t and p_r.

Differential derivatives of density, radial pressure, and transverse pressure are shown in Figs. 4, 5 and 6. For all three models and strange compact stars, we observe that $0 > \frac{d\rho}{dr}$, $0 > \frac{dp_r}{dr}$, and $0 > \frac{dp_t}{dr}$. When $r = 0$, we obtain,

$$0 = \frac{d\rho}{dr}$$

$$0 = \frac{dp_r}{dr}$$

As expected, we have a maximum density for minuscule r (star core density $\rho(0) = \rho_c$), as these are decreasing functions.

6.2 Energy conditions

The Raychaudhuri expansion equation [52] provides the generic form of the energy conditions. These circumstances lead one to conclude that gravity's attracting character and positive energy density prevent it from flowing faster than the speed of light. Reference [53] provides a thorough discussion of the strong energy conditions (SEC) and null energy conditions (NEC).

- **NEC** (Null Energy Condition): $\rho_{\text{mat}} + p_{rad} \geq 0$, $\rho_{\text{mat}} + p_{tan} \geq 0$
- **WEC** (Weak Energy Condition): $\rho_{\text{mat}} \geq 0$, $p_{rad} \geq 0$, $p_{tan} \geq 0$
- **SEC** (Strong Energy Condition): $\rho_{\text{mat}} + p_{rad} \geq 0$, $\rho_{\text{mat}} + p_{tan} \geq 0$, $\rho_{\text{mat}} + p_{rad} + 2p_{tan} \geq 0$
- **DEC** (Dominant Energy Condition): $\rho_{\text{mat}} \geq |p_{rad}|$, $\rho_{\text{mat}} \geq |p_{tan}|$

Our viable models have been shown to satisfy any of these energy constraints for compact stars, as shown graphically in Figs. 7, 8 and 9.

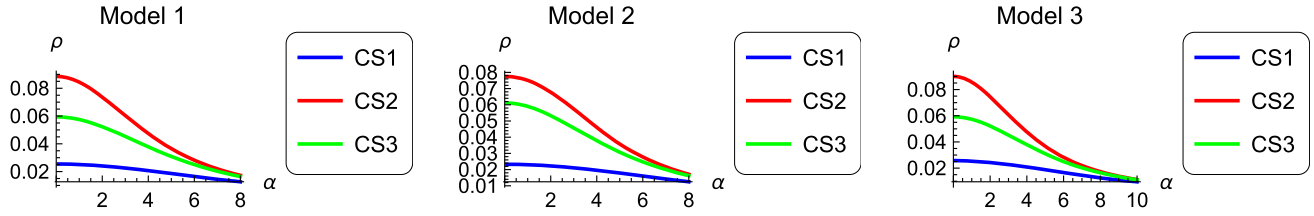

Fig. 1 Density evolution for three different models of strange star candidates (Her X-1, SAX J1808.4-3658, and 4U 1820-30) under modified $f(R)$ gravity. The impact of parameter choices ($\alpha = 0.03$, $\beta = 0.3$, and $\gamma = 0.5$) on the density profiles is demonstrated, ensuring the satisfaction of energy conditions and stability criteria across all models

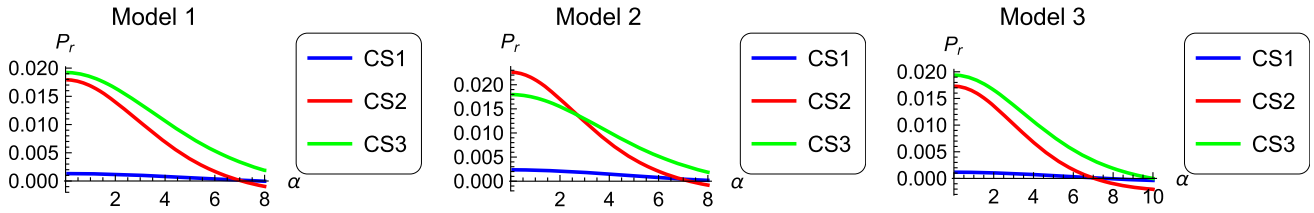

Fig. 2 Evolution of radial pressure for three different models of strange star candidates (Her X-1, SAX J1808.4-3658, and 4U 1820-30) under modified $f(R)$ gravity. The effects of parameter choices ($\alpha = 0.03$, $\beta = 0.3$, and $\gamma = 0.5$) on the radial pressure profiles are shown

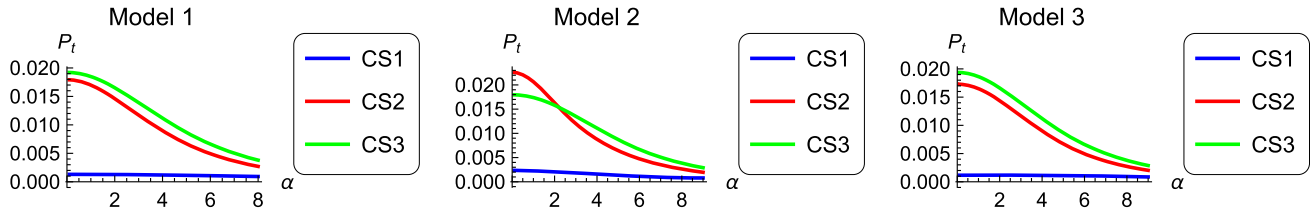

Fig. 3 Evolution of transverse pressure for three different models of strange star candidates (Her X-1, SAX J1808.4-3658, and 4U 1820-30) under modified $f(R)$ gravity. The effects of parameter choices ($\alpha = 0.03$, $\beta = 0.3$, and $\gamma = 0.5$) on the transverse pressure profiles are demonstrated

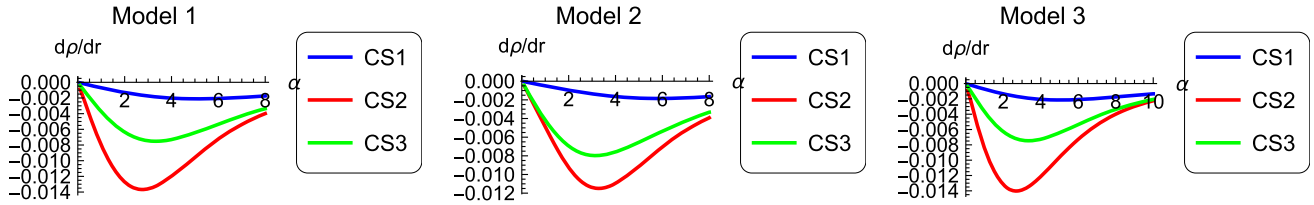

Fig. 4 Evolution of $\frac{d\rho}{dr}$ for three different models of strange star candidates (Her X-1, SAX J1808.4-3658, and 4U 1820-30) under modified $f(R)$ gravity as r increases. The effects of parameter choices ($\alpha = 0.03$, $\beta = 0.3$, and $\gamma = 0.5$) are shown

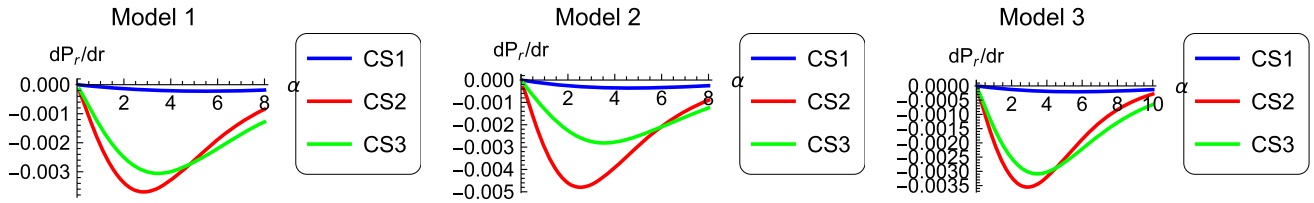

Fig. 5 Evolution of $\frac{dP_r}{dr}$ for three different models of strange star candidates (Her X-1, SAX J1808.4-3658, and 4U 1820-30) under modified $f(R)$ gravity as r increases. The effects of parameter choices ($\alpha = 0.03$, $\beta = 0.3$, and $\gamma = 0.5$) are shown

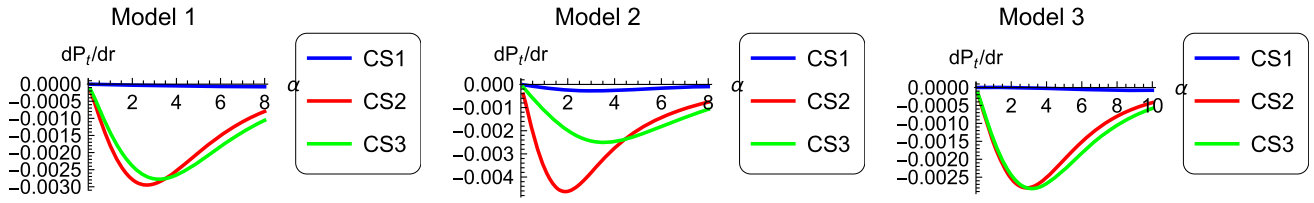

Fig. 6 Evolution of $\frac{dP_t}{dr}$ for three different models of strange star candidates (Her X-1, SAX J1808.4-3658, and 4U 1820-30) under modified $f(R)$ gravity as r increases. The effects of parameter choices ($\alpha = 0.03$, $\beta = 0.3$, and $\gamma = 0.5$) are shown

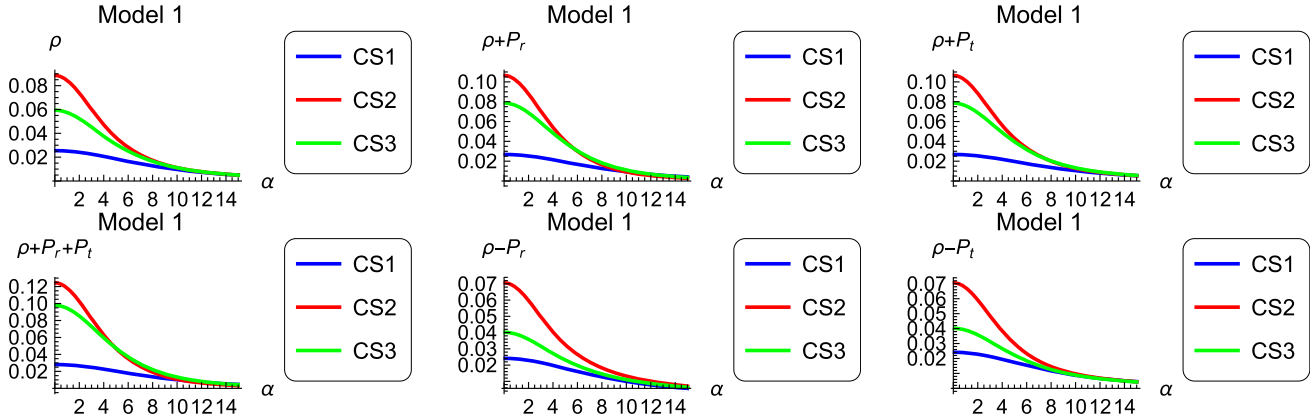

Fig. 7 Energy conditions for strange star candidates under Model 1 of modified $f(R)$ gravity, demonstrating the impact of the parameter choice $\alpha = 0.03$

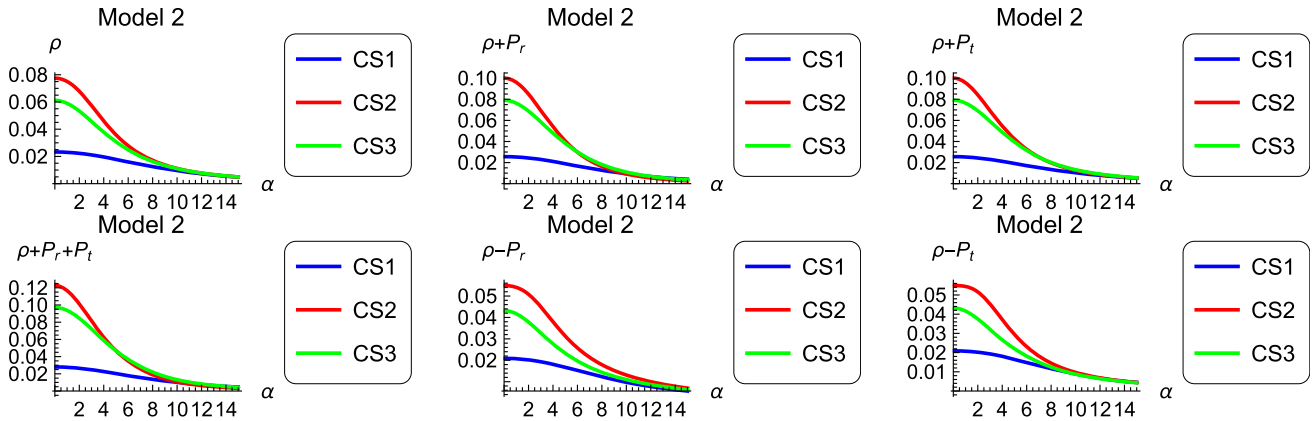

Fig. 8 Energy conditions for strange star candidates under Model 2 of modified $f(R)$ gravity, demonstrating the impact of parameter choices $\alpha = 0.03$ and $\gamma = 0.5$

6.3 Tolman–Oppenheimer–Volkoff (TOV) equation

Equation (7) provides a Tolman–Oppenheimer–Volkoff (TOV) equation for a spherically symmetric anisotropic stellar interior. The first metric coefficient of the line element contains the function whose radial derivative is assigned to the term a. a is in general related to the scalar component of the four accelerations ($a^\beta = aV^\beta$) of anisotropic fluid.

The term on the right side of Equation (22) can be recast as its hydrostatic (F_h), anisotropic (F_a), and gravitational (F_g) components. These forces' values are obtained as follows for the anisotropic spherical matter distribution:

These definitions are used in Fig. 10 to show how the forces behave for three compact stars at the beginning of hydrostatic equilibrium. We go further in our analysis with these graphs and extend it to other $f(R)$ gravity models. Fig 10 shows the variations from Model 1 in the left panel, Model 2 in the middle panel, and their corresponding variations of principal forces for Model 3 in the right panel.

$$-\frac{B\sqrt{C}r(P_r+\rho)}{A+\frac{1}{2}B\sqrt{C}r^2}+\frac{dP_r}{dr}+\frac{2(P_r-P_t)}{r}=0 \tag{17}$$

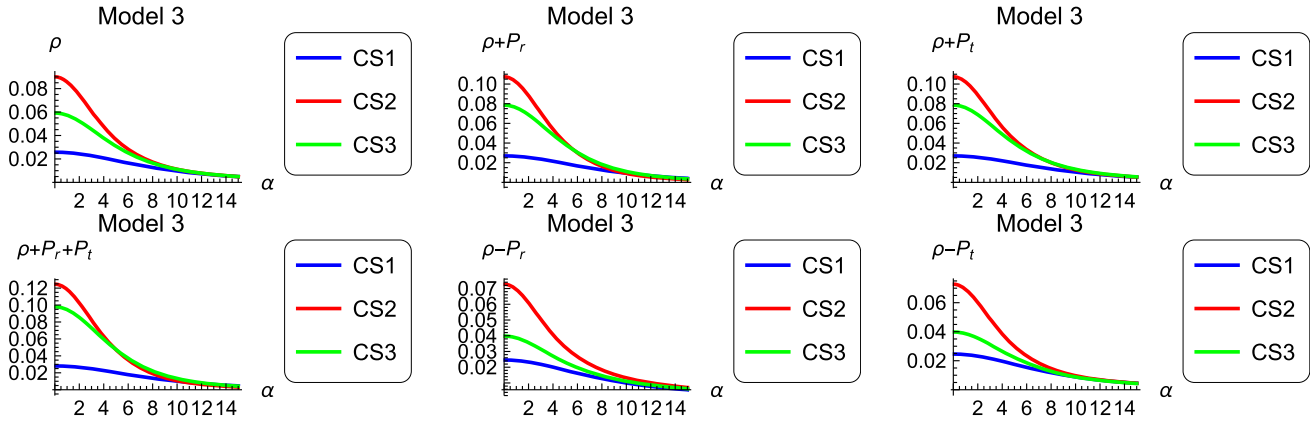

Fig. 9 Energy conditions for strange star candidates under Model 3 of modified $f(R)$ gravity, demonstrating the impact of parameter choices $\alpha = 0.03$, $\beta = 0.3$, and $\gamma = 0.5$

Additionally, it can be expressed as hydrostatic, anisotropic, and gravitational forces.

$$F_g + F_a + F_h = 0, \tag{18}$$

which produces

$$F_g = -\frac{B\sqrt{cr}\,(P_r + \rho)}{A + \frac{1}{2}B\sqrt{cr^2}},$$
$$F_a = \frac{2(p_r - p_t)}{r}, F_h = -\frac{dp_r}{dr}$$

As shown in Fig. 10, we use these concepts to plot for 3 strange compact stars.

where the radial coordinate α affects the gravitational force (F_g), hydrostatic force (F_h), and anisotropic force (F_a). The plots of Models 1, 2, and 3 are on the left, middle, and right, respectively.

6.4 Analysis of stability

Here, we assess the stability of our stellar models using Herrera's [54] method, which is predicated on the notion of cracking (or overturning). The closed interval [0, 1] must contain both the squared transverse sound speed v_{st}^2 and the squared radial sound speed v_{sr}^2. Here, the transverse sound speed is indicated by v_{st} and the radial sound speed is represented by v_{sr}.

The system needs to meet the criterion $v_{st}^2 > v_{sr}^2$ in order to be dynamically stable. For all three kinds of weird stars, the evolution of the transverse and radial sound velocity has been found to stay inside the stability constraints in some areas. All of our star configurations (in the framework of the $f(R)$ models) meet this restriction, as illustrated in Fig. 11.

We therefore draw the conclusion that, under this theoretical framework, all of our suggested models are stable. Sharif and Yousaf [55], who used a different mathematical approach to analyze compact star objects, have achieved similar results.

$$\frac{dp_r}{d\rho} = v_{sr}^2$$

and

$$\frac{dp_t}{d\rho} = v_{st}^2$$

Both the transverse and radial speeds must adhere to the criterion for stability. At least $0 \le v_{sr}^2 \le 1$ and $0 \le v_{st}^2 \le 1$

As illustrated in Figs. 11 and 12, the radial and transversal speed of sound evolutions for all three categories of odd star candidates are within the investigated stability bounds.

Similarly, Fig. 13 shows that

$$0 < |v_{st}^2 - v_{sr}^2| < 1$$

Thus, in $f(R)$ gravity models, stability is achieved for compact stars.

6.5 EoS parameter

The state of matter under particular physical conditions is described by the equation of state (EoS) parameter, a dimensionless variable. Usually falling inside the open interval (0, 1), this parameter indicates a cosmic epoch dominated by radiation. One definition of the EoS for an anisotropic relativistic interior is as follows:

The graphic representation of ω_r for our compact structures can be found in Fig. 14. Every compact structure that is being considered exhibits a similar trend for ω_t. The criterion $0 < \omega_r < 1$ is satisfied for compact objects with a maximum radius of about $r \sim (\le 7)$ (CS Radius), but the constraint $0 < \omega_t < 1$ is valid for any higher value of r. In the vicinity of the core region, this suggests that $\omega_i > 1$. The spherically symmetric self-gravitating system is located at the matching

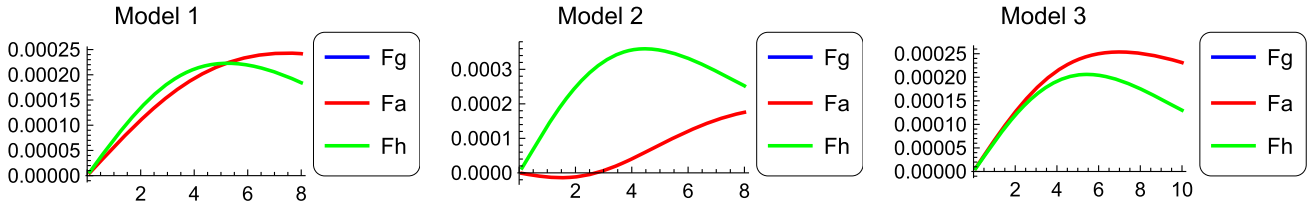

Fig. 10 Variation of the anisotropic force F_a, hydrostatic force F_h, and gravitational force F_g with respect to the radial coordinate r for strange star candidates under modified $f(R)$ gravity, demonstrating the effects of parameter choices $\alpha = 0.03$, $\beta = 0.3$, and $\gamma = 0.5$

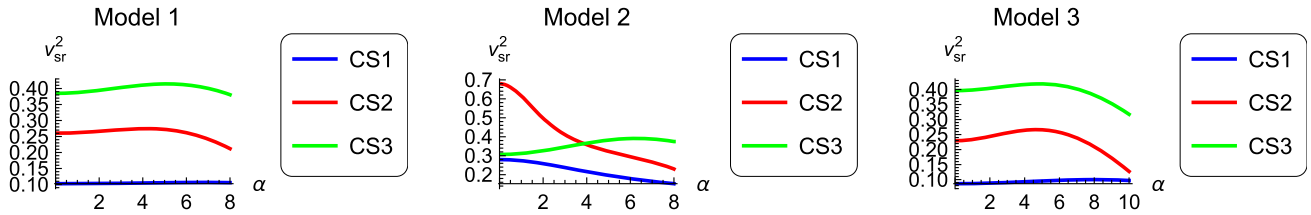

Fig. 11 Variation of the radial sound speed v_{sr}^2 for strange star candidates under modified $f(R)$ gravity, demonstrating the effects of parameter choices $\alpha = 0.03$, $\beta = 0.3$, and $\gamma = 0.5$

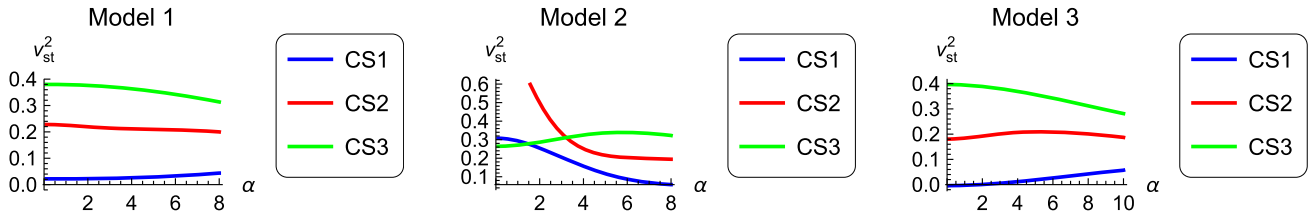

Fig. 12 Variation of the transverse sound speed v_{st}^2 for strange star candidates under modified $f(R)$ gravity, demonstrating the effects of parameter choices $\alpha = 0.03$, $\beta = 0.3$, and $\gamma = 0.5$

hypersurfaces within a radiation window. It follows that the inside of our relativistic bodies is compact.

$$p_r = w_r \rho$$

$$p_t = w_t \rho.$$

For example, $0 < w_r < 1$ and $0 < w_t < 1$ are examples of limitations. Figures 14 and 15 provide a graphic representation of the behavior of w_r and w_t.

In which we can see that $0 < w_r < 1$ and $0 < w_t < 1$ which suggests that the matter content is usual real matter.

6.6 The anisotropy measurement

We evaluate the level of anisotropy in relativistic interior modeling in this section. The anisotropy in a stellar system can be quantified using the following formula:

ϵ is directly connected to the difference $p_t - p_r$. The anisotropic pressure is directed outward when ϵ is positive, meaning that $p_t > p_r$. On the other hand, if it ϵ is negative, the pressure is directed inside. Our systems' anisotropy factor, which we calculated, was $\epsilon > 0$, showing that $p_t > p_r$. Figure 16 illustrates these findings.

$$\Delta = \frac{2}{r}(p_t - p_r) \tag{19}$$

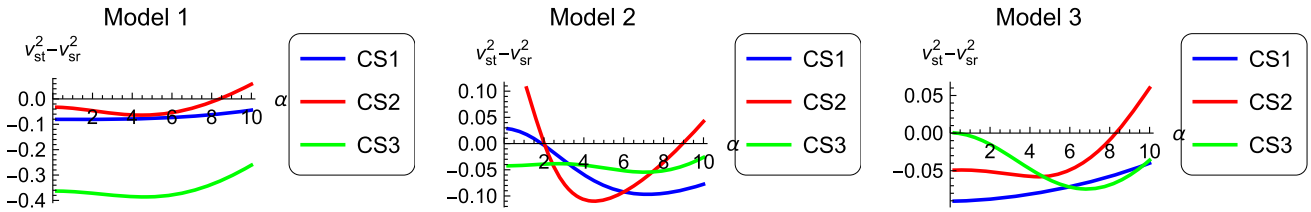

Fig. 13 Variation of $v_{st}^2 - v_{sr}^2$ for strange star candidates under modified $f(R)$ gravity, demonstrating the effects of parameter choices $\alpha = 0.03$, $\beta = 0.3$, and $\gamma = 0.5$

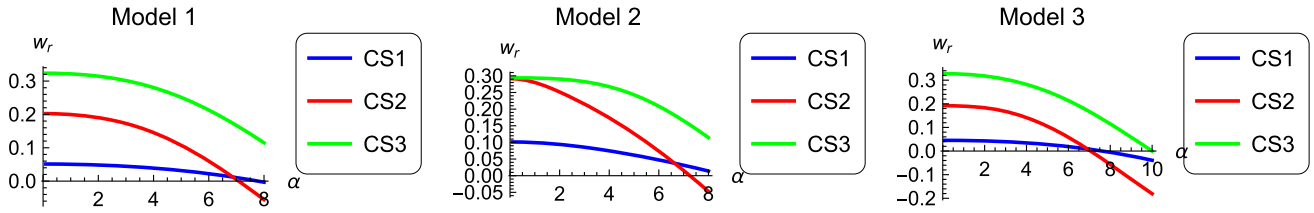

Fig. 14 Variation of the radial equation of state (EoS) parameter with respect to the radial coordinate for strange star candidates under modified $f(R)$ gravity, demonstrating the effects of parameter choices $\alpha = 0.03$, $\beta = 0.3$, and $\gamma = 0.5$

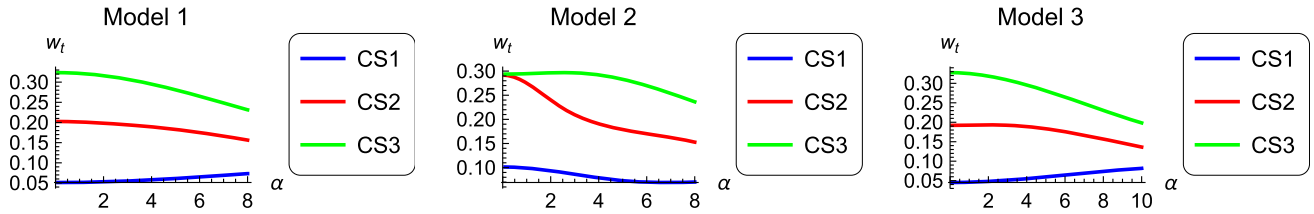

Fig. 15 Variation of the transverse equation of state (EoS) parameter with respect to the radial coordinate for strange star candidates under modified $f(R)$ gravity, demonstrating the effects of parameter choices $\alpha = 0.03$, $\beta = 0.3$, and $\gamma = 0.5$

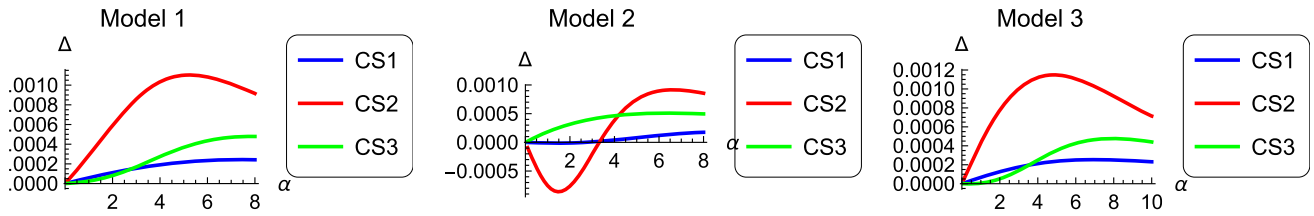

Fig. 16 Variation of the anisotropic measure Δ with respect to the radial coordinate for strange star candidates under modified $f(R)$ gravity, demonstrating the effects of parameter choices $\alpha = 0.03$, $\beta = 0.3$, and $\gamma = 0.5$

Plotting the anisotropy yields $\Delta > 0$, i.e., $p_t > p_r$, indicating that the anisotropy measure is outward directed. Figure 16 displays these plots.

7 Summary

This paper aims to investigate the physical properties of spherically symmetric compact stars in the framework of f(R) metric gravity. By matching the interior solutions with a suitable exterior solution at the boundary surface, the Krori-Barua solutions explain the metric functions of a spherically symmetric star, and the arbitrary constants are determined. It is possible to explain these random constants in terms of the mass and radius of any compact star. Utilizing observational data from three distinct star models and three physically plausible $f(R)$ gravity models, we investigate the impact of the additional degrees of freedom introduced by $f(R)$ gravity. By altering the parameters of the stellar and gravity models, we plot the material variables, including anisotropic stresses and energy density, as functions of radial distance.

We show that the energy density declines with increasing star radius, indicating a maximally dense arrangement in the stellar interior. Both tangential and radial pressure evolution show a similar pattern. Except for the tangential pressure derivative in the compact star Her X-1, which remains positive until $R = 4.8$ before going negative, it is found that for each of the three models, the radial derivatives of these material variables decrease with increasing radius. Notably, the first derivatives of these material variables vanish at $r = 0$ for every compact star that is part of the analysis.

The analysis confirms that our spherically symmetric anisotropic systems satisfy the weak, null, strong, and dominant energy criteria, thus validating the physical validity of these compact stars under the influence of the extra degrees of freedom provided by fourth-order gravity. Our findings further demonstrate the collapsing character of these relativistic star formations by demonstrating that gravitational forces outweigh the corresponding repulsive forces. It is known that if the radial and tangential sound velocity stay within the range [0, 1], then the stellar system is stable against perturbations. It was discovered, meanwhile, that the compact star Her X-1 does not uphold this criterion under the second gravity model. However, while the tangential sound speed v_t^2 is greater than the radial sound speed v_r^2, Fig. 11 shows that all of the stellar models are stable. Furthermore, the anisotropy parameter stays positive and the equation of state parame-

ter for all compact stars falls inside the range (0, 1), both of which are necessary for actual stellar configurations.

It is important to note that the limitations of this study arise from the specific assumptions and conditions imposed by the chosen $f(R)$ gravity models and Finch–Skea spacetime. Similar studies on charged compact stars in $f(G)$ gravity have demonstrated the sensitivity of structural properties to modifications in the gravitational action [56]. Furthermore, the existence of anisotropic self-gravitating systems under different $f(R)$ models has shown that anisotropy plays a crucial role in determining the stability and physical behavior of compact stars [57]. Additionally, the incorporation of a variable cosmological constant in $f(R, T)$ gravity provides further insights into how modified gravity theories can influence the internal structure and equation of state of compact stars [58].

Acknowledgements This work was supported and funded by the Deanship of Scientific Research at Imam Mohammad Ibn Saud Islamic University (IMSIU) (Grant number IMSIU-DDRSP2503).

Data Availability Statement This manuscript has no associated data. [Author's comment: Data sharing not applicable to this article as no datasets were generated or analysed during the current study.].

Code Availability Statement This manuscript has no associated code/software. [Author's comment: Code/Software sharing not applicable to this article as no code/software was generated or analysed during the current study.].

Open Access This article is licensed under a Creative Commons Attribution 4.0 International License, which permits use, sharing, adaptation, distribution and reproduction in any medium or format, as long as you give appropriate credit to the original author(s) and the source, provide a link to the Creative Commons licence, and indicate if changes were made. The images or other third party material in this article are included in the article's Creative Commons licence, unless indicated otherwise in a credit line to the material. If material is not included in the article's Creative Commons licence and your intended use is not permitted by statutory regulation or exceeds the permitted use, you will need to obtain permission directly from the copyright holder. To view a copy of this licence, visit http://creativecommons.org/licenses/by/4.0/.
Funded by SCOAP[3].

References

1. S. Weinberg, The cosmological constant problem. Rev. Mod. Phys. **61**(1), 1 (1989)
2. P. James, E. Peebles, B. Ratra, The cosmological constant and dark energy. Rev. Mod. Phys. **75**(2), 559 (2003)
3. V. Husain, B. Qureshi, Ground state of the universe and the cosmological constant. A nonperturbative analysis. Phys. Rev. Lett. **116**(6), 061302 (2016)
4. D. Pietrobon, A. Balbi, D. Marinucci, Integrated Sachs-Wolfe effect from the cross correlation of WMAP 3 year and the NRAO VLA sky survey data: new results and constraints on dark energy. Phys. Rev. D Part. Fields Gravit. Cosmol. **74**(4), 043524 (2006)
5. T. Giannantonio, R.G. Crittenden, R.C. Nichol, R. Scranton, G.T. Richards, A.D. Myers, R.J. Brunner, A.G. Gray, A.J. Connolly, D.P. Schneider, High redshift detection of the integrated Sachs–Wolfe effect. Phys. Rev. D Part. Fields Gravit. Cosmol. **74**(6), 063520 (2006)
6. A.G. Riess, L.-G. Strolger, S. Casertano, H.C. Ferguson, B. Mobasher, B. Gold, P.J. Challis, A.V. Filippenko, S. Jha, W. Li et al., New Hubble space telescope discoveries of type Ia supernovae at z = 1: narrowing constraints on the early behavior of dark energy. Astrophys. J. **659**(1), 98 (2007)
7. A. Qadir, H.W. Lee, K.Y. Kim, Modified relativistic dynamics. Int. J. Mod. Phys. D **26**(05), 1741001 (2017)
8. S. Nojiri, S.D. Odintsov, Modified gravity with negative and positive powers of curvature: unification of inflation and cosmic acceleration. Phys. Rev. D **68**(12), 123512 (2003)
9. S. Nojiri, S.D. Odintsov, V.K. Oikonomou, Modified gravity theories on a nutshell: inflation, bounce and late-time evolution. Phys. Rep. **692**, 1–104 (2017)
10. R.F. Sawyer, Condensed π - phase in neutron-star matter. Phys. Rev. Lett. **29**(6), 382 (1972)
11. L. Herrera, N.O. Santos, A. Wang, Shearing expansion-free spherical anisotropic fluid evolution. Phys. Rev. D Part. Fields Gravit. Cosmol. **78**(8), 084026 (2008)
12. L. Herrera, G. Le Denmat, N.O. Santos, Expansion-free evolving spheres must have inhomogeneous energy density distributions. Phys. Rev. D Part. Fields Gravit. Cosmol. **79**(8), 087505 (2009)
13. A. Di Prisco, L. Herrera, J. Ospino, N.O. Santos, V.M. Viña-Cervantes, Expansion-free cavity evolution: some exact analytical models. Int. J. Mod. Phys. D **20**(12), 2351–2367 (2011)
14. Z. Yousaf, K. Bamba, M.Z.H. Bhatti, Role of tilted congruence and f (R) gravity on regular compact objects. Phys. Rev. D **95**(2), 024024 (2017)
15. Z. Yousaf, M.Z.H. Bhatti, Cavity evolution and instability constraints of relativistic interiors. Eur. Phys. J. C **76**, 1–15 (2016)
16. M. Sharif, Z. Yousaf, Radiating cylindrical gravitational collapse with structure scalars in f (R) gravity. Astrophys. Space Sci. **357**, 1–11 (2015)
17. R.A. Sussman, L.G. Jaime, Lemaître–Tolman–Bondi dust solutions in f (R) gravity. Class. Quantum Gravity **34**(24), 245004 (2017)
18. Z. Yousaf, M.Z.H. Bhatti, Electromagnetic field and cylindrical compact objects in modified gravity. Mon. Not. R. Astron. Soc. **458**(2), 1785–1802 (2016)
19. M. Sharif, Z. Yousaf, Dynamics of spherical stars with structure scalars and R + R n cosmology. Can. J. Phys. **93**(8), 905–911 (2015)
20. Hamid Shabani and Amir Hadi Ziaie, Stability of the Einstein static universe in f (R, T) gravity. Eur. Phys. J. C **77**, 1–15 (2017)
21. F. Rajabi, K. Nozari, Unimodular $f(R, T)$ gravity. Phys. Rev. D **96**(8), 084061 (2017)
22. R. Garattini, G. Mandanici, Rainbow's stars. Eur. Phys. J. C **77**, 1–13 (2017)
23. P.K. Sahoo, P. Sahoo, B.K. Bishi, Anisotropic cosmological models in f (R, T) gravity with variable deceleration parameter. Int. J. Geom. Methods Mod. Phys. **14**(06), 1750097 (2017)
24. S.K. Sahu, S.K. Tripathy, P.K. Sahoo, A. Nath, Cosmic transit and anisotropic models in f (R, T) gravity. Chin. J. Phys. **55**(3), 862–869 (2017)
25. S.W. Hawking, G.F.R. Ellis, *The Large Scale Structure of Space-time* (Cambridge University Press, Cambridge, 2023)
26. L. Herrera, N.O. Santos, Local anisotropy in self-gravitating systems. Phys. Rep. **286**(2), 53–130 (1997)
27. A. Di Luis Herrera, J.L.H.-P. Prisco, N.O. Santos, On the role of density inhomogeneity and local anisotropy in the fate of spherical collapse. Phys. Lett. A **237**(3), 113–118 (1998)
28. M. Zaeem-ul Haq Bhatti, Z. Yousaf, S. Hanif, Gravitational collapse in generalized teleparallel gravity. Eur. Phys. J. Plus **132**(5), 230 (2017)

29. G.J. Olmo, Limit to general relativity in f (R) theories of gravity. Phys. Rev. D Part. Fields Gravit. Cosmol. **75**(2), 023511 (2007)
30. F. Briscese, E. Elizalde, Black hole entropy in modified-gravity models. Phys. Rev. D Part. Fields Gravit. Cosmol. **77**(4), 044009 (2008)
31. A. de La Cruz-Dombriz, A.A.L.M. Dobado, A.L. Maroto, Black holes in f (R) theories. Phys. Rev. D Part. Fields Gravit. Cosmol. **80**(12), 124011 (2009)
32. T. Clifton, P.G. Ferreira, A. Padilla, C. Skordis, Modified gravity and cosmology. Phys. Rep. **513**(1–3), 1–189 (2012)
33. S. Capozziello, M. De Laurentis, S.D. Odintsov, A. Stabile, Hydrostatic equilibrium and stellar structure in f (R) gravity. Phys. Rev. D Part. Fields Gravit. Cosmol. **83**(6), 064004 (2011)
34. M. De Salvatore Capozziello, I.D. Laurentis, M.F. Martino, S.D. Odintsov, Jeans analysis of self-gravitating systems in f (R) gravity. Phys. Rev. D Part. Fields Gravit. Cosmol. **85**(4), 044022 (2012)
35. J.A.R. Cembranos, A. De la Cruz-Dombriz, B.M. Nunez, Gravitational collapse in f (R) theories. J. Cosmol. Astropart. Phys. **2012**(04), 021 (2012)
36. M. Sharif, Z. Yousaf, Instability of meridional axial system in f (R) gravity. Eur. Phys. J. C **75**, 1–15 (2015)
37. M. Sharif, Z. Yousaf, Cylindrical thin-shell wormholes in f (R) gravity. Astrophys. Space Sci. **351**, 351–360 (2014)
38. M. Sharif, Z. Yousaf, Charged adiabatic ltb gravitational collapse in f (R) gravity. Int. J. Theor. Phys. **55**, 470–480 (2016)
39. M. Zaeem Ul Haq Bhatti, Z. Yousaf, Influence of electric charge and modified gravity on density irregularities. Eur. Phys. J. C **76**, 1–13 (2016)
40. Z. Yousaf, M. Bhatti, U. Farwa, Stability of compact stars in αr 2+ β (r $\gamma\delta$t $\gamma\delta$) gravity. Mon. Not. R. Astron. Soc. **464**, 4509–4519 (2017)
41. M. Zaeem-ul-Haq Bhatti, Z. Yousaf, S. Hanif, Role of f (T) gravity on the evolution of collapsing stellar model. Phys. Dark Universe **16**, 34–40 (2017)
42. M.R. Finch, J.E.F. Skea, A realistic stellar model based on an ansatz of Duorah and Ray. Class. Quantum Gravity **6**(4), 467 (1989)
43. T. Gangopadhyay, S. Ray, X.-D. Li, J. Dey, M. Dey, Strange star equation of state fits the refined mass measurement of 12 pulsars and predicts their radii. Mon. Not. R. Astron. Soc. **431**(4), 3216–3221 (2013)
44. T. Güver, F. Özel, A. Cabrera-Lavers, P. Wroblewski, The distance, mass, and radius of the neutron star in 4u 1608–52. Astrophys. J. **712**(2), 964 (2010)
45. A.A. Starobinsky, A new type of isotropic cosmological models without singularity. Phys. Lett. B **91**(1), 99–102 (1980)
46. E. Guido Cognola, S.N. Elizalde, S.D. Odintsov, L. Sebastiani, S. Zerbini, Class of viable modified f (R) gravities describing inflation and the onset of accelerated expansion. Phys. Rev. D Part. Fields Gravit. Cosmol. **77**(4), 046009 (2008)
47. K. Bamba, C.-Q. Geng, C.-C. Lee, Cosmological evolution in exponential gravity. J. Cosmol. Astropart. Phys. **2010**(08), 021 (2010)
48. N. Itoh, Hydrostatic equilibrium of hypothetical quark stars. Prog. Theor. Phys. **44**(1), 291–292 (1970)
49. E. Witten, Cosmic separation of phases. Phys. Rev. D **30**(2), 272–285 (1984)
50. H.A. Buchdahl, General relativistic fluid spheres. Phys. Rev. **116**(4), 1027–1034 (1959)
51. H. Bondi, Massive spheres in general relativity. Proc. R. Soc. Lond. Ser. A Math. Phys. Sci. **282**(1389), 303–317 (1964)
52. A. Raychaudhuri, Relativistic cosmology. I. Phys. Rev. **98**(4), 1123–1126 (1955)
53. S.W. Hawking, G.F.R. Ellis, *The Large Scale Structure of Space-Time* (Cambridge University Press, Cambridge, 1973)
54. L. Herrera, J. Jimenez, M. Esculpi, Surface phenomena in general relativistic stellar models: critical mass and stability. Phys. Lett. A **130**(4–5), 211–216 (1988)
55. M. Sharif, Z. Yousaf, Dynamical analysis of self-gravitating stars in f (R, T) gravity. Astrophys. Space Sci. **354**, 471–479 (2014)
56. M. Ilyas, Charged compact stars in $f(G)$ gravity. Eur. Phys. J. C **78**(9), 757 (2018)
57. Z. Yousaf, M. Sharif, M. Ilyas, M.Z. Bhatti, Influence of $f(R)$ models on the existence of anisotropic self-gravitating systems. Eur. Phys. J. C **77**, 1–10 (2017)
58. M. Ilyas, Compact stars with variable cosmological constant in $f(R, T)$ gravity. Astrophys. Space Sci. **365**(11), 180 (2020)